

Cobalt-Catalyzed Selective Oxidation of the Tertiary Phosphane Triphos with Molecular Oxygen[☆]

Katja Heinze, Gottfried Huttner* and Laszlo Zsolnai

University of Heidelberg, Department of Inorganic Chemistry,
Im Neuenheimer Feld 270, D-69120 Heidelberg, Germany
Fax: (internat.) + 49(0)6221/545707
E-mail: katja@sun0.urz.uni-heidelberg.de

Received June 10, 1997

Keywords: Tripod ligands / Phosphane oxides / Cobalt / Oxidation / Catalysis

The reactivity of complexes of triphos [$\text{CH}_3\text{C}(\text{CH}_2\text{PPh}_2)_3$] and CoCl_2 towards dioxygen has been investigated. Reaction of the pseudo-tetrahedral complex $(\eta^2\text{-triphos})\text{CoCl}_2$ (**1**) with dioxygen yields after work-up the mixed phosphane/phosphane oxide ligands triphosO and triphosO₂. The novel ligand triphosO₂ can be obtained in quantitative yield using catalytic amounts of **1**. In order to gain some insight into the catalytic dioxygen activation reaction, experiments with va-

rious triphos/Co/Cl species, in different solvents and at several concentrations have been carried out. A mechanism involving two separate reaction pathways is proposed. Complexes of triphosO and triphosO₂ with CoCl_2 , $[\eta^2\text{-}(P,P)\text{-triphosO}]\text{CoCl}_2$ (**4**), and $[\eta^2\text{-}(P,O)\text{-triphosO}_2]\text{CoCl}_2$ (**5**), which are present as intermediates in the oxygenation reaction, have been isolated and fully characterized including X-ray structural analyses.

Introduction

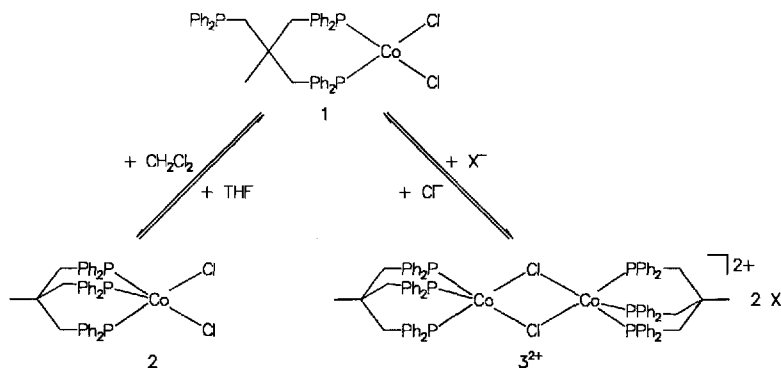
The oxidation of tertiary phosphanes to phosphane oxides is well-known in synthetic chemistry.^[1] This may be accomplished by reaction of the phosphane with KMnO_4 ,^[2] H_2O_2 ,^[3] or OPCl_3 .^[4] Trialkylphosphanes are susceptible to autoxidation yielding a mixture of all possible $\text{R}_n\text{PO}(\text{OR})_{3-n}$ products ($\text{R} = \text{alkyl}$).^[5] Furthermore, triphenylphosphane can be oxidized to triphenylphosphane oxide by metal-catalyzed reaction with dioxygen.^[6] Polytertiary phosphanes are oxidized by H_2O_2 ^[7] or OPCl_3 ^[4] to the corresponding polyphosphane oxides. Oxidation of polytertiary phosphanes to mixed phosphanes/phosphane oxides by using a small amount of oxidizing agent results in a mixture of all possible products and unreacted starting compounds. Specifically, the tritertiary phosphane triphos [$\text{CH}_3\text{C}(\text{CH}_2\text{PPh}_2)_3$] is oxidized to a mixture of triphosO_{*n*} ($n = 0-3$).^[8]

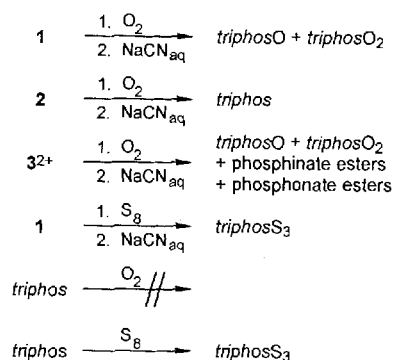
In order to study the reactivity of complexes of triphos with CoCl_2 (Scheme 1) towards group-VI elements, the complexes $(\eta^2\text{-triphos})\text{CoCl}_2$ (**1**)^[9], $(\eta^3\text{-triphos})\text{CoCl}_2$ (**2**)^[9], and $[(\eta^3\text{-triphos})\text{Co}(\mu\text{-Cl})_2\text{Co}(\eta^3\text{-triphos})] \cdot (\text{BPh}_4)_2$ [**3** · $(\text{BPh}_4)_2$]^{[9][10]} (Scheme 1) were allowed to react with O_2 and S_8 , respectively. Analysis of the products obtained and variation of the reaction conditions allowed us to develop a catalytic and selective method for synthesizing the mixed phosphane/phosphane oxide triphosO₂ [$\text{CH}_3\text{C}(\text{CH}_2\text{PPh}_2)(\text{CH}_2\text{P}(\text{O})\text{Ph}_2)_2$] in high yields, and to design a route for preparing the mixed phosphane/phosphane oxide triphosO [$\text{CH}_3\text{C}(\text{CH}_2\text{PPh}_2)_2(\text{CH}_2\text{P}(\text{O})\text{Ph}_2)$].

Results and Discussion

Depending on the reaction conditions, different products are obtained from the reaction of CoCl_2 with triphos, namely the blue high-spin complex **1** and the red low-spin

Scheme 1. Complexes of Co^{II} with chloride and triphos



Scheme 2. Reactions with O₂ and S₈

complexes **2** and **3**²⁺ (Scheme 1).^[9] These complexes were found to react with various Lewis acids and Lewis bases yielding addition and substitution products, respectively.^[9] Additionally, the reduced complex η^3 -triphosCo^ICl and the oxidized complex $[\eta^3\text{-triphosCo}^{\text{II}}\text{Cl}_2]^+$ could be prepared.^[9]

The products obtained after work-up of reactions of **1**, **2**, and **3**²⁺ with dioxygen (see Experimental Section) are compiled in Scheme 2. The five-coordinate complex **2** was found to be unreactive towards O₂, while the tetrahedral high-spin complex **1** and the dinuclear complex **3**²⁺ yield oxygenated triphos ligands (Table 1, Scheme 2): **1** gives the phosphane oxides triphosO and triphosO₂ (and no triphosO₃, which was prepared for comparison purposes by oxidation of triphos with H₂O₂; Table 1), while **3**²⁺ additionally produces significant amounts of higher oxygenated products (phosphinate and phosphonate esters of triphos). Reaction of **1** with S₈ yields the trisulfide triphosS₃

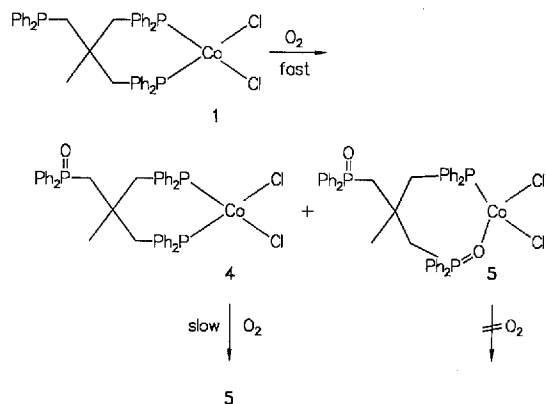
(Table 1, Scheme 2). From these observations it is inferred that different mechanisms are operative in the various reactions. As shown in Scheme 2, a metal complex is not necessary to form triphosS₃ from triphos and S₈. Clearly, the S–S bonds of S₈ are easily broken to form sulfur radicals, which attack the phosphane [$E_{\text{diss}}(\text{S}_8) = 226 \text{ kJ mol}^{-1}$].^[11] Therefore, no selectivity is observed in the reaction of **1** with S₈. In the oxygenation reaction, however, the cobalt ion seems to be essential for the reaction to occur since triphos does not react with O₂ under these conditions [$E_{\text{diss}}(\text{O}_2) = 493 \text{ kJ mol}^{-1}$]^[11] (Scheme 2). The dinuclear complex **3**²⁺ is known to dissociate easily into reactive 15 VE species $[(\eta^3\text{-triphos})\text{CoCl}]^+$, which can be trapped as $[(\eta^3\text{-triphos})\text{CoCl}(\text{L})]^+$ (L = CO, PMe₃, NH₃, CH₃CN).^[9] A reactive dioxygen adduct is possibly formed, which unselectively attacks the phosphane groups to form phosphane oxides and higher oxygenated products.

In the reaction of **1** with O₂ it was possible to detect intermediates, namely the complexes $[\eta^2\text{-}(P,P)\text{-triphosO}]\text{-CoCl}_2$ (**4**) and $[\eta^2\text{-}(P,O)\text{-triphosO}_2]\text{CoCl}_2$ (**5**) (Scheme 3). Both could be isolated as blue (**4**) and light-blue (**5**) powders. Their composition was determined by conductivity and magnetic susceptibility measurements, UV/Vis/NIR and IR spectroscopy, mass spectrometry (Table 2), as well as by X-ray crystallographic analyses. Both these intermediates were found to be non-conducting, high-spin complexes (Table 2). The UV/Vis/NIR spectra of **1** and **4** (Figure 1) are very similar. Hence, a similar ligand field (2 × P and 2 × Cl) must be present, implying a coordination of the triphosO ligand via two phosphane groups, with the phosphane oxide group remaining non-coordinated. The UV/Vis spectrum of **5**, on the other hand, although showing the

Table 1. ¹H-, ³¹P-, ¹³C-NMR, and IR data of triphosO_n (n = 1, 2, 3) and triphosS₃

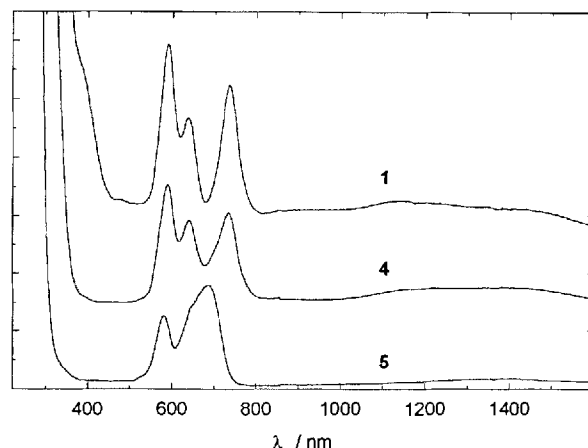
	triphosO	triphosO ₂	triphosO ₃	triphosS ₃
¹ H NMR				
CH ₃	1.05 (s, 3 H)	1.01 (s, 3 H)	0.94 (s, 3 H)	0.70 (s, 3 H)
CH ₂	2.5–2.7 (m, 6 H)	2.8–3.1 (m, 6 H)	3.22 (d, 6 H) ^[a]	3.79 (d, 6 H) ^[b]
CH _{ar}	7.2–7.7 (m, 30 H)	7.3–7.8 (m, 30 H)	7.4–7.8 (m, 30 H)	7.5–8.1 (m, 30 H)
³¹ P NMR				
P	–24.1 (s, 2 P)	–23.7 (s, 1 P)	–	–
P=X	29.1 (s, 1 P) ^[c]	30.2 (s, 2 P) ^[c]	31.0 (s) ^[c]	36.1 (s) ^[d]
¹³ C NMR				
CH ₃	29.7 (m)	29.7 (m)	29.1 (q) ^[e]	26.4 (q) ^[e]
CH ₂ P	43.7 (m)	44.5 (m)	–	–
CH ₂ P=X	41.0 (m)	41.2 (m)	41.1 (tvd) ^[f]	41.8 (tvd) ^[g]
C _{cl}	39.9 (m)	39.9 (m)	39.7 (q) ^[h]	42.3 (q) ^[h]
C _{ipso} P	139.9 (dvd) ^[i]	139.7 (d) ^[i]	–	–
C _{ortho} P	133.5 (dvd) ^[j]	133.5 (d) ^[i]	–	–
C _{meta} P	128.9 (s)	129.0 (s)	–	–
C _{para} P	128.9 (s)	129.0 (s)	–	–
C _{ipso} P=X	135.8 (d) ^[m]	135.5 (d) ^[m]	135.1 (d) ^[m]	134.3 (d) ^[n]
C _{ortho} P=X	130.9 (d) ^[o]	131.0 (d) ^[o]	130.9 (d) ^[o]	131.6 (d) ^[p]
C _{meta} P=X	128.9 (d) ^[q]	128.9 (d) ^[q]	129.0 (d) ^[q]	128.9 (d) ^[q]
C _{para} P=X	131.6 (bs)	131.7 (bs)	131.8 (bs)	131.6 (bs)
IR				
$\tilde{\nu}(\text{P=X}) [\text{cm}^{-1}]$	1193 (st)	1184 (st)	1181 (st)	622 (st), 610 (st)

^[a] ²J(P–CH₂) = 10.6 Hz. – ^[b] ²J(P–CH₂) = 11.6 Hz. – ^[c] ¹J(P–CH₂) = 69 Hz; ¹J(P–C_{ipso}) = 98 Hz. – ^[d] ¹J(P–CH₂) = 47 Hz; ¹J(P–C_{ipso}) = 80 Hz. – ^[e] ³J(P–CH₃) = 5.5 Hz. – ^[f] ¹J(P–CH₂) = 68.9 Hz; ³J(P'–CH₂) = 6.4 Hz. – ^[g] ¹J(P–CH₂) = 47.8 Hz; ³J(P'–CH₂) = 6.4 Hz. – ^[h] ²J(P–C_{cl}) = 4.6 Hz. – ^[i] ¹J(P–C_{ipso}) = 12.8 Hz; ³J(O=P'–C_{ipso}) = 7.3 Hz. – ^[j] ¹J(P–C_{ipso}) = 11.0 Hz. – ^[k] ²J(P–C_{ortho}) = 20.0 Hz; ⁶J(O=P'–C_{ortho}) = 5.6 Hz. – ^[l] ²J(P–C_{ortho}) = 19.3 Hz. – ^[m] ¹J(P–C_{ipso}) = 98.2 Hz. – ^[n] ¹J(P–C_{ipso}) = 80.9 Hz. – ^[o] ²J(P–C_{ortho}) = 9.2 Hz. – ^[p] ²J(P–C_{ortho}) = 10.1 Hz. – ^[q] ³J(P–C_{meta}) = 12.0 Hz.

Scheme 3. Reactions of (triphosO_n)CoCl₂ with O₂ (*n* = 0, 1, 2)

typical splitting of a pseudo-tetrahedral Co^{II} complex, is different from those of **1** and **4**, ruling out P₂Cl₂ coordination in this instance. An O₂Cl₂ coordination can also be excluded as the absorption bands of **5** (Table 2) are shifted relative to those of (dpppO₂)CoCl₂ [dpppO₂ = 1,3-bis(diphenylphosphoryl)propane] ($\lambda = 588, 649, 667 \text{ nm}$)^[12]. Therefore, a mixed P₂OCl₂ coordination seems to be present in **5**, with the second P=O group of the ligand being non-coordinated. The presence of dangling phosphane oxide groups in **4** and **5** is further supported by the IR spectra, which show unshifted P=O stretching frequencies compared to the free ligands (Tables 1 and 2). From the electronic spectra of the complexes **4** and **5** it is possible to estimate the ligand field parameters Δ and B' ^[13]: $\Delta = 4680 \text{ cm}^{-1}$ (**4**) and 4280 cm^{-1} (**5**); $B' = 550 \text{ cm}^{-1}$ (**4**), and 629 cm^{-1} (**5**). As expected, two phosphane groups induce a stronger ligand field splitting and allow for a larger delocalization of the electrons than a mixed phosphane/phosphane oxide donor set

Complex **4** crystallized from THF/Et₂O with an additional CoCl₂ fragment bridging two molecules of **4** via the dangling phosphane oxide groups, thus forming a trinuclear aggregate (Figure 2). Both crystallographically independent fragments of **4** exhibit similar geometries, so that the discussion will be restricted to just one of the molecular units (Co1 in Figure 2). As deduced from the analytical data

Figure 1. UV/Vis spectra of **1**, **4** and **5** in THF

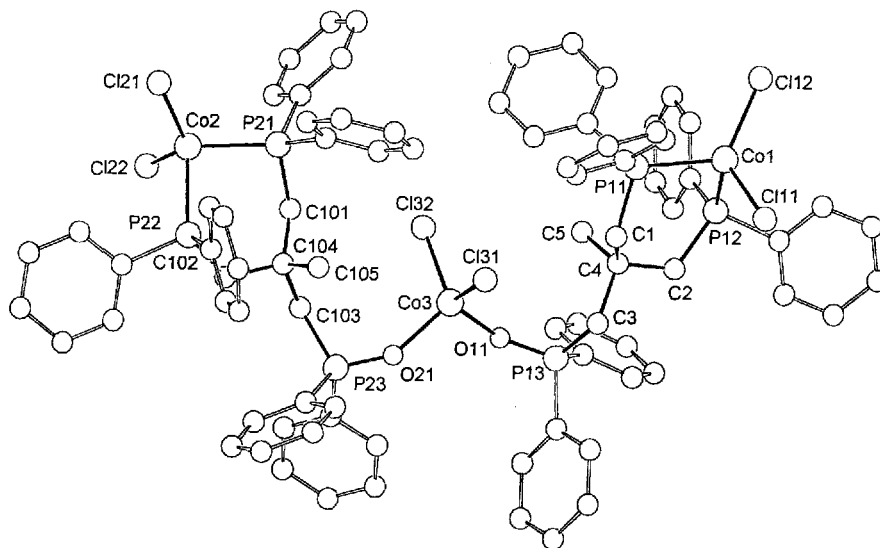
(vide supra), the triphosO ligand coordinates via its two phosphane groups at the cobalt center. The six-membered chelate ring thus formed (Co1–P11–C1–C4–C2–P12) adopts a slightly distorted chair conformation (alternating signs of the six torsion angles^[14]) similar to that of the analogous (dppp)CoCl₂ complex [dppp = 1,3-bis(diphenylphosphano)propane]^[9]. The Co–P and Co–Cl bond lengths of **4** (Table 3) are also comparable to those of the (dppp)CoCl₂ complex.^[9] The geometry around the metal center is pseudo-tetrahedral with a small P–Co–P and a large Cl–Co–Cl angle, the RMS deviation from an ideal tetrahedral arrangement being 10°. ^[15] The deviation is twice as large as that of the “bridging” CoCl₂ fragment (Co3, Figure 2), which is not involved in a chelate ring system. The P–O bond lengths of the phosphane oxide groups that are coordinated at the central cobalt (Co3) are not significantly larger than those of non-coordinating P=O groups (vide infra), indicating only a small decrease in the P–O bond order and thus a weak Co–O bond (Table 3). Complexes of the triphosO ligand have been prepared previously with Rh^{III}^[8], Rh^{III}^[16], Ni^{II}^[17], and Re^I^[18]; in all cases the P=O group remains non-coordinating.

The triphosO₂ complex **5** crystallizes in the centrosymmetric space group *P* $\bar{1}$ with two independent molecules of

Table 2. Selected analytical data of **4**, **5**, and **7** · (BPh₄)

	4	5	7 · (BPh ₄)
λ_{max} [nm] (ϵ [l mol ⁻¹ cm ⁻¹])	589 (390), 644 (330), 705 (260, sh), 733 (300), 1276 (80, br) ^[a]	582 (250), 648 (290), 688 (360), 1370 (30, br) ^[a]	435 (895), 641 (425), 745 (250, sh), 889 (90, sh), 1426 (50, br.) ^[b]
Λ_{M} [S cm ² mol ⁻¹]	< 0.5 ^[a]	< 0.5 ^[a]	27 ^[b]
$\mu_{\text{eff}}/\mu_{\text{B}}$ (295 K)	4.1 ^[a]	4.3 ^[a]	2.2 ^[b]
<i>m/z</i> (%) [fragment]	734 (100) [M – Cl] ⁺ , 640 (18) [M – CoCl ₂] ⁺ , 563 (63) [M – CoCl ₂ – Ph] ⁺	750 (7) [M – Cl] ⁺ , 656 (40) [M – CoCl ₂] ⁺ , 579 (100) [M – CoCl ₂ – Ph] ⁺	363 (2) [M – Cl] ⁺ , 242 (100) [BPh ₃] ⁺ , 164 (70) [BPh ₂] ⁺ , 944 (s, P–CH ₃)
$\tilde{\nu}$ [cm ⁻¹]	1191 (m, P=O)	1187 (w, P=O), 1167 (m, P=O)	

[^a] In THF. – [^b] In CH₂Cl₂.

Figure 2. View of the trinuclear unit of $(4)_2 \cdot \text{CoCl}_2$ 

5 and three solvent molecules in the unit cell. As the two complex molecules are very similar, the discussion will be confined to just one of them (Figure 3). The triphosO₂ ligand coordinates via one phosphane and one phosphane oxide group at the cobalt center, forming a seven-membered chelate ring (Co1–P1–C1–C4–C2–P2–O2). When the triphosO₂ ligand coordinates, its C_s symmetry is lost and the C4 atom of the neopentane backbone becomes an asymmetric center [Figure 3 shows the (*S*) enantiomer]. The geometry around the metal center is pseudo-tetrahedral with only minor deviations from an ideal tetrahedral arrangement (the RMS deviation being only 5°^[15]). This is certainly a result of the smaller ring strain of the seven-membered chelate ring as compared to that of the six-membered ring in **4** (vide supra). The P=O bond length of the coordinated phosphane oxide group is only marginally larger than that of the dangling P=O group, again indicating a weak Co–O bond (Table 4).

The complexes **1**, **4**, and **5** show varying reactivity towards dioxygen (Scheme 3): Complex **1** reacts readily with O₂ giving the complexes **4** and **5**; **4** is slowly oxidized

to **5** over a period of several hours, while **5** remains inert towards O₂ for at least 24 h. These observations explain the fact that no triphosO₃ is observed as a product in the oxygenation reaction.

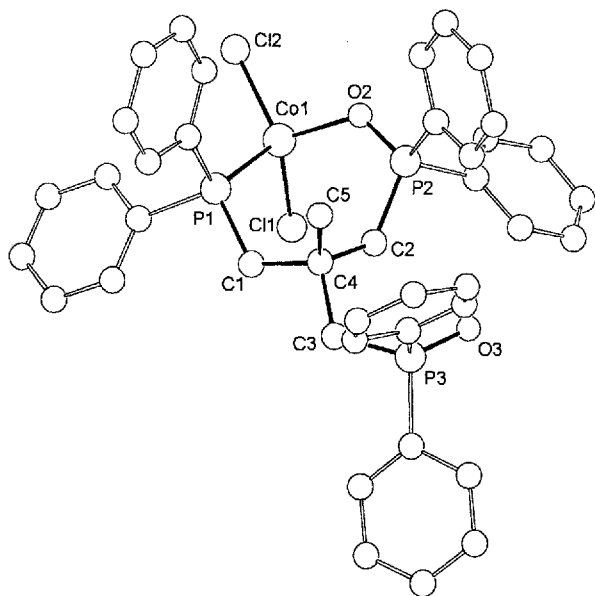
To investigate whether unsaturated species arising from chloride dissociation might be involved in the reaction, the complexes were treated with NaBPh₄ (Scheme 4). Complex **1** reacts with NaBPh₄ to form the dinuclear complex **3**²⁺ (Schemes 1 and 4)^{[9][10]}, while both oxygenated complexes **4** and **5** are stable with regard to chloride loss with Na⁺ as the chloride acceptor. Clearly, the dangling phosphane oxide arms of the ligands in **4** and **5** are unable to coordinate the metal so as to compensate for the chloride abstraction. These facts, together with the different products observed in the oxygenation with **3**²⁺, render the participation of intermediates of the type [(triphosO_{*n*})CoCl]⁺ (*n* = 0, 1, 2) unlikely.

As tetrahedral phosphane complexes of Co^{II}, i.e. [(PR₃)₂CoCl₂], are known to undergo equilibria of the type (PR₃)₂CoCl₂ + PR₃ ⇌ (PR₃)₃CoCl₂^[19], analogous reactions of **1**, **4**, and **5** with PMe₃ were investigated. Complex

Table 3. Selected bond lengths [Å]^[a] and angles [°]^[a] of $(4)_2 \cdot \text{CoCl}_2$

Co1		Co2		Co3	
Co1–Cl11	2.236(3)	Co2–Cl22	2.241(3)	Co3–Cl31	2.255(3)
Co1–Cl12	2.209(3)	Co2–Cl21	2.208(3)	Co3–Cl32	2.246(3)
Co1–P11	2.341(3)	Co2–P21	2.338(3)	Co3–O11	1.992(7)
Co1–P12	2.342(3)	Co2–P22	2.345(3)	Co3–O21	1.984(7)
				P13–O11	1.507(7)
				P23–O21	1.509(7)
Cl11–Co1–Cl12	118.7(1)	Cl21–Co2–Cl22	122.3(1)	Cl31–Co3–Cl32	109.6(1)
P11–Co1–P12	96.4(1)	P21–Co2–P22	96.2(1)	O11–Co3–O21	108.9(3)
Cl11–Co1–P11	101.9(1)	Cl22–Co2–P21	104.1(1)	Cl31–Co3–O11	115.7(2)
Cl12–Co1–P11	119.0(1)	Cl21–Co2–P21	117.1(1)	Cl32–Co3–O11	103.6(2)
Cl11–Co1–P12	100.3(1)	Cl22–Co2–P22	96.4(1)	Cl31–Co3–O21	103.6(2)
Cl12–Co1–P12	116.6(1)	Cl21–Co2–P22	116.0(1)	Cl32–Co3–O21	115.9(2)
				Co3–O11–P13	137.6(5)
				Co3–O21–P23	140.7(5)

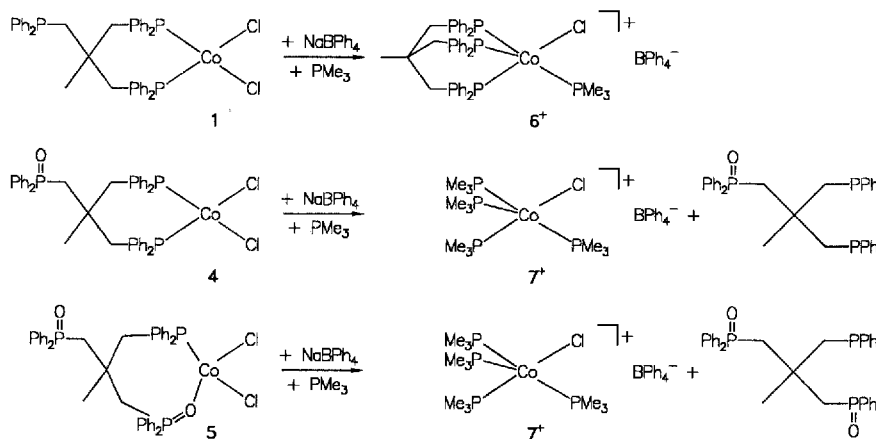
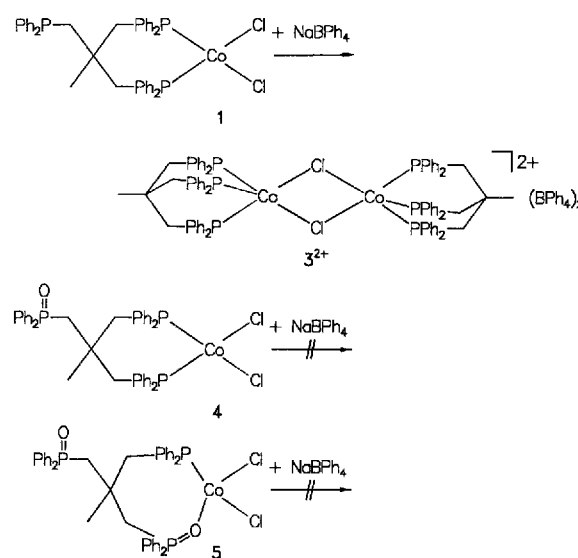
^[a] Estimated standard deviations of the least significant figures are given in parentheses.

Figure 3. View of the molecular structure of **5** (molecule A)Table 4. Selected bond lengths [\AA]^[a] and angles [$^\circ$]^[a] of **5**

	molecule A	molecule B
Co1–Cl1	2.245(3)	2.246(3)
Co1–Cl2	2.219(3)	2.227(3)
Co1–P1	2.373(3)	2.369(3)
Co1–O2	1.977(5)	1.976(6)
P2–O2	1.507(6)	1.511(6)
P3–O3	1.487(6)	1.491(6)
Cl1–Co1–Cl2	116.7(1)	116.9(1)
Cl1–Co1–P1	110.26(9)	102.9(1)
Cl2–Co1–P1	113.5(1)	113.5(1)
Cl1–Co1–O2	113.5(2)	113.2(2)
Cl2–Co1–O2	109.3(2)	110.1(2)
P1–Co1–O2	102.6(2)	98.7(2)
Co1–O2–P2	126.9(3)	127.2(3)

^[a] Estimated standard deviations of the least significant figures are given in parentheses.

1 gives the known air-stable, five-coordinate complex **6**⁺[9], while addition of PMe_3 to solutions of **4** and **5** leads to complete displacement of the triphos O_n ligands ($n = 1, 2$)

Scheme 5. Reactions of $(\text{triphosO}_n)\text{CoCl}_2$ with PMe_3 ($n = 0, 1, 2$)Scheme 4. Reactions of $(\text{triphosO}_n)\text{CoCl}_2$ with NaBPh_4 ($n = 0, 1, 2$)

yielding complex **7**⁺ (Scheme 5). These reactions suggest that intermediate five-coordinate species might in principle exist and, furthermore, they emphasize the high lability of the oxygenated ligands in **4** and **5**.

The cationic complex **7**⁺ has been prepared previously as the BF_4^- salt and its structure has been determined by X-

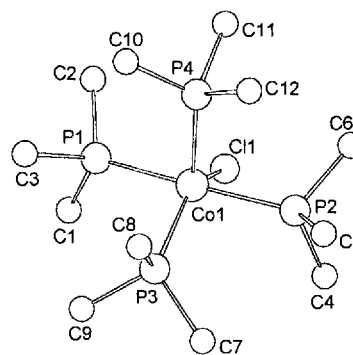
Figure 4. View of the molecular structure of the cation of **7**· (BPh_4) 

Table 5. Selected bond lengths [\AA]^[a] and angles [$^\circ$]^[a] of $7 \cdot (\text{BPh}_4)$

$7 \cdot (\text{BPh}_4)$					
Co1–Cl1	2.278(1)	P1–Co1–P2	169.83(5)	P3–Co1–P4	108.67(5)
Co1–P1	2.251(1)	P1–Co1–P3	93.21(5)	Cl1–Co1–P1	84.68(4)
Co1–P2	2.256(1)	P1–Co1–P4	92.32(5)	Cl1–Co1–P2	85.19(5)
Co1–P3	2.259(1)	P2–Co1–P3	93.50(5)	Cl1–Co1–P3	136.69(5)
Co1–P4	2.285(1)	P2–Co1–P4	92.77(5)	Cl1–Co1–P4	114.64(5)

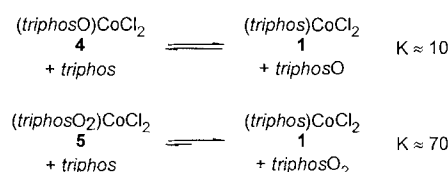
^[a] Estimated standard deviations of the least significant figures are given in parentheses.

ray crystallography. As the crystals of the BF_4^- salt were of “poor quality”^[19a], we determined the solid-state structure of the BPh_4^- salt (Figure 4, Table 5). The geometry of the complex cation can be described as distorted trigonal-bipyramidal, with P1 and P2 occupying axial coordination sites and the Cl atom lying in an equatorial position. Interestingly, the geometry of 7^+ is very similar to that found in 6^+ ^[9], in spite of the fact that in 7^+ only monodentate phosphanes coordinate at the cobalt center.

The lability of the ligands triphosO_n ($n = 1, 2$) in their cobalt chloride complexes **4** and **5** is not only evident from the ease of their displacement by PMe_3 , but also from the ligand exchange reactions of **4** and **5** with triphos (Scheme 6).^[20] The reactions show that displacement of the triphosO_n ligands ($n = 1, 2$) by triphos is not only kinetically possible, but is also thermodynamically favoured, especially in complex **5**, which has one weak $\text{P}=\text{O} \rightarrow \text{Co}$ bond.

In an attempt to understand some of the finer details of the formation of the two phosphane oxides triphosO_n ($n = 1, 2$) and eventually to optimize the relative yields of these products, several experiments using different solvents, reaction times and concentrations were carried out (Table 6).

Scheme 6. Ligand exchange of $(\text{triphosO}_n)\text{CoCl}_2$ with triphos ($n = 1, 2$)



Experiments concerning different complexes of triphos with CoCl_2 (Table 6, runs 1–4) have already been summarized in Scheme 2 (vide supra). The implication of these was that the primary active species is the four-coordinate complex **1**. Using different solvents, in which only the tetrahedral complex **1** is present, such as THF, acetone or benzene^[9], does not drastically affect the product distribution; in all cases nearly equal amounts of triphosO and triphosO_2 were obtained (Table 6, runs 4–6). These experiments suggest that solvent coordination and participation of the solvent in the oxygen transfer reaction play only minor roles. Additionally, the solvent acting as an oxygen acceptor can also be ruled out as the amount of dioxygen consumed dur-

Table 6. Product distribution of the aerobic oxidation of triphos

run	complex ^[a]	triphos [$\times 10^{-2}$ M]	time [h]	solvent	yield (%) triphos	triphosO	triphosO_2
1	–	2.50	5.00	THF	100	0	0
2	2	2.50	5.00	CH_2Cl_2	91	9	<1
3	3 ²	2.50	5.00	THF	0	17	83 ^[b]
4	1	2.50	5.00	THF	0	45	55
5	1	2.50	5.00	acetone	0	38	62
6	1	2.50	5.00	benzene	0	50	50
7	1	2.50	0.25	THF	80	15	5
8	1	2.50	0.50	THF	69	24	7
9	1	2.50	1.00	THF	49	35	16
10	1	2.50	2.00	THF	25	46	29
11	1	2.50	4.00	THF	4	48	48
12	1	2.50	6.00	THF	0	44	56
13	1	2.50	8.00	THF	0	42	58
14	1	2.50	12.00	THF	0	40	60
15	1	5.00	5.00	THF	0	50	50
16	1	2.50	5.00	THF	0	45	55
17	1	0.25	5.00	THF	0	0	100
18 ^[c]	1	10.00	5.00	THF	0	45	55
19 ^[c]	1	5.00	5.00	THF	0	23	77
20 ^[c]	1	2.00	5.00	THF	0	11	89
21 ^[c]	1	1.00	5.00	THF	0	4	96
22 ^[c]	1	0.50	5.00	THF	0	0	100
23	4	2.50	5.00	THF	–	91	9

^[a] 10 mol-% (based on Co). – ^[b] + Phosphinate and phosphonate esters; signals in the ^{31}P -NMR spectrum: $\delta = -4.2, -8.8, -10.4, -16.2, -21.1, -21.2, -21.8, -22.6$. – ^[c] In 20 ml of THF.

ing the reaction (as determined manometrically) corresponds to that found in the oxygenated ligands (consumed: 2.2 ± 0.2 mmol O; found: 2.4 ± 0.1 mmol O).

To monitor the progress of the reaction, samples were withdrawn from the reaction mixture at timed intervals and analyzed for their relative content of the phosphane oxides (Table 6, runs 7–14). The results are depicted graphically in Figure 5. A typical ^{31}P -NMR spectrum of the products (after work-up, see Experimental Section) is shown in Figure 6, from which the product distribution can easily be determined. The concentration of the educt triphos decreases exponentially, that of triphosO increases quite rapidly during the first two hours and thereafter slowly decreases again, while the yield of triphosO₂ continuously increases (Figure 5). At first sight, the rates of formation are suggestive of a simple consequent reaction $\text{A} \rightarrow \text{B} \rightarrow \text{C}$ with B (= triphosO) being an intermediate. However, if this were the case one would expect the concentration of B to

reach a maximum value at some time and then to decrease to zero thereafter. This is clearly not the case as the intermediate B accumulates quite rapidly as long as there is excess triphos present, and it is only slowly converted into the final product C (= triphosO₂) as all the triphos is consumed (Figure 5). On the other hand, two simple parallel reactions $\text{A} \rightarrow \text{B}$ and $\text{A} \rightarrow \text{C}$ should give simple exponential rises of the two products B and C , which is not observed either. Both reaction types together, the consequent and the parallel, however, can account for the observed rates of formation: the two parallel reactions with rate constants of similar magnitude (under the conditions applied) and a much slower consequent reaction. The latter can be observed separately in the reaction of complex **4** with O₂ (Scheme 3). The conversion is only about 10% after 5 h (Table 6, run 23), implying a slower reaction of **4** with O₂ compared to that of **1** (100% conversion; 5 h; Table 6, run 4).

The product distribution depends not only on the reaction time, but also on the concentration of the reactants. The concentration of triphos was varied from 0.25×10^{-2} to $10 \times 10^{-2} \text{ M}^{[21]}$; the concentration of Co^{II} being 10 mol-% (Table 6, runs 15–22). As is apparent from Figure 7, the yield of triphosO₂ is quantitative at low concentrations and the yield of triphosO increases with concentration. These findings show that the relative rates of the two parallel reactions can be influenced by varying the concentration. The increased formation of triphosO at higher concentrations might be the result of a bimolecular reaction pathway involving a dinuclear complex as a transition state or short-lived intermediate. A similar mechanistic interpretation was previously suggested for the oxidation of (PEt₃)₂CoCl₂, leading to (OPEt₃)(PEt₃)CoCl₂ and (OPEt₃)₂CoCl₂.^[22]

These experiments, together with the observation that the oxygenated ligands triphosO_{*n*} (*n* = 1, 2) are easily displaced by triphos (vide supra), allow the formulation of a catalytic

Figure 5. Time-dependent product distribution

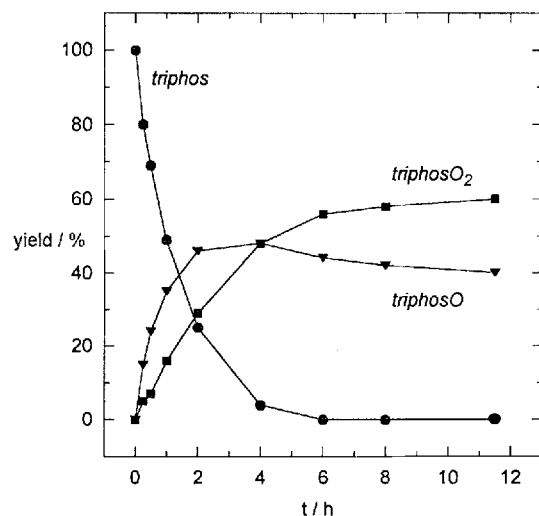
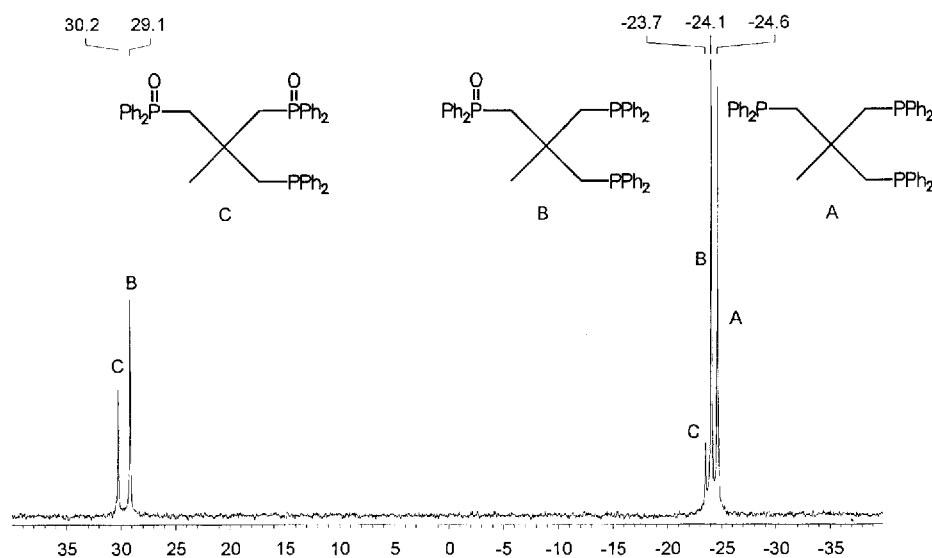


Figure 6. ^{31}P -NMR spectrum of the products obtained after 2h



reaction pathway involving two parallel reactions and a slow consequent reaction. The proposed catalytic cycles are depicted in Scheme 7. The first step is necessarily the formation of a dioxygen adduct of **1**, which unfortunately could not be observed using EPR techniques, although numerous examples of mononuclear dioxygen adducts of Co^{II} are known in the literature.^[23] At this point of the reaction, either an intramolecular rearrangement to complex **5** takes place (Scheme 7, left pathway) or, at high concentrations of **1**, a bimetallic dioxygen adduct^{[23d][23e][23f][23g][23h][23i][23j][23k]} is formed, which subsequently undergoes the oxygen transfer reaction and dissociation forming complex **4** (Scheme 7, right pathway). The active complex **1** is then formed once more by displacement of the ligands triphosO_n from the complexes **4** ($n = 1$) and **5** ($n = 2$), respectively, by triphos.

The present study of the reaction of **1** with dioxygen has illustrated that it is possible to selectively oxidize triphos at one or two phosphane groups, to give the mixed ligands triphosO and triphosO₂. These could be prepared in analytically pure form and in fairly good and quantitative yields, respectively. The coordination behaviour of the triphosO ligand towards Co^{II} corresponds to that reported previously in the literature for other metal ions; the com-

plexation properties of the novel ligand triphosO₂ towards Co^{II} have been investigated. Experiments are presently being carried out with the aim of preparing complexes of the triphosO₂ ligand with metal ions in high oxidation states.

This work received support from the *Deutsche Forschungsgemeinschaft*, the *Fonds der Chemischen Industrie* and the *Volkswagen-Stiftung*.

Experimental Section

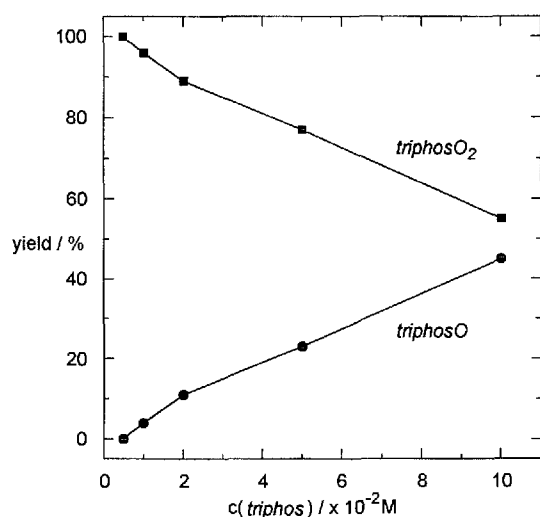
General Methods: Unless noted otherwise, all manipulations were carried out under an inert atmosphere by means of standard Schlenk techniques. All solvents were dried by standard methods and distilled under inert gas. The chromatography was performed on deaerated silica gel (ICN, particle size 32–63 μm). – NMR: Bruker AC 200 at 200.13 MHz (¹H), 50.323 MHz (¹³C{¹H}), 81.015 MHz (³¹P{¹H}); chemical shifts (δ) in ppm with respect to $\text{CHCl}_3/\text{CDCl}_3$ (¹H: $\delta = 7.24$, ¹³C: $\delta = 77.0$) as internal standard and to H_3PO_4 (³¹P: $\delta = 0$) as external standard. – IR: Bruker FTIR IFS-66, as CsI disks. – UV/Vis/NIR: Perkin-Elmer Lambda 19. – MS: Finnigan MAT 8230. – EPR: Bruker ESP 300 E, X-band, standard cavity ER 4102, temperature control unit Eurotherm B-VT 2000, external standard diphenylpicrylhydrazyl (DPPH). – Elemental analyses: Microanalytical laboratory of the Organisch-Chemisches Institut, University of Heidelberg. – Melting points: Gallenkamp MFB-595 010, uncorrected values. – Cyclic voltammetry: Metrohm “Universal Meß- und Titriergefäß”, Metrohm GC electrode RDE 628, platinum electrode, SCE electrode, Princeton Applied Research potentiostat Model 273, 10^{-3} M in 0.1 M *n*Bu₄NPF₆/CH₂Cl₂. – Magnetic susceptibility measurements (Evans method): Calibration with diphenylpicrylhydrazyl (DPPH)^[24]. – Conductance measurements: Schott conductivity bridge CG 855 in ca. 10^{-3} M solutions.

Chemicals: 1,1,1-Tris(diphenylphosphanomethyl)ethane, $\text{CH}_3\text{C}(\text{CH}_2\text{PPh}_2)_3$ ^[25], CoCl_2 ^[26].

Crystallographic Structure Determinations: The measurements were carried out on a Siemens P4 (Nicolet Syntex) R3m/v four-circle diffractometer with graphite-monochromated Mo- K_α radiation. All calculations were performed using the SHELXT-PLUS software package. Structures were solved by direct methods with the SHELXS-86 program and refined with the SHELXL-93 program.^[27] Graphics were prepared using XPLA and ZORTEP.^[28] An absorption correction (ψ scan, $\Delta\psi = 10^\circ$) was applied to all data. Atomic coordinates and anisotropic thermal parameters of the non-hydrogen atoms were refined by a full-matrix least-squares calculation. Compound **4**: All phenyl rings were treated as rigid bodies of D_{6h} symmetry; the THF solvate molecule was found to be disordered over two orientations with s.o.f.s of 0.5; all solvent molecules (THF, Et₂O) were refined isotropically. Compound **5**: The acetone solvent molecules were found to be distributed over four sites with s.o.f.s of 0.75. Compound **7** (BPh_4): Rotational disorder was observed for the chlorine atoms of the CH_2Cl_2 molecule with s.o.f.s of 0.7, 0.2, and 0.1. Data relating to the structure determinations is compiled in Table 7. Further details of the crystal structure determinations may be obtained from the Fachinformationszentrum Karlsruhe, D-76344 Eggenstein-Leopoldshafen (Germany), on quoting the depository numbers CSD-407076 (**4**), -407079 (**5**) and -407075 [**7** (BPh_4)].

General Procedure for the Oxidation of Triphos: In a typical experiment, 1 mmol of triphos (624 mg) and 0.1 mmol of CoCl_2 (13 mg) were dissolved in THF (40 ml), if necessary by sonicating the initial suspension. The blue solution was poured into a beaker

Figure 7. Concentration-dependent product distribution



Scheme 7. Proposed catalytic oxygenation cycle of triphos with CoCl_2

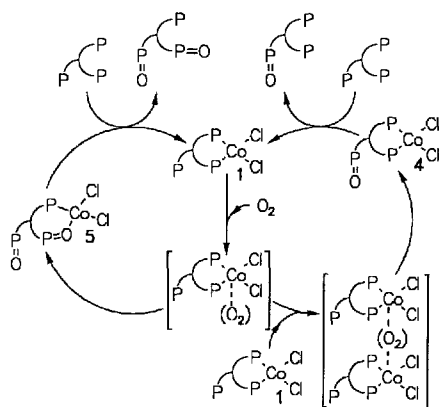


Table 7. Crystallographic data of (4)₂·CoCl₂, 5, and 7·(BPh₄)

	(4) ₂ ·CoCl ₂	5	7·(BPh ₄)
formula	C ₈₂ H ₇₈ Cl ₆ Co ₃ O ₂ P ₆ · 1 Et ₂ O · 1.5 THF	C ₄₁ H ₃₀ Cl ₂ CoO ₂ P ₃ · 1.5 (CH ₃) ₂ CO	C ₃₆ H ₅₆ BClCoP ₄ · 1 CH ₂ Cl ₂
M _r [g mol ⁻¹] (without solvates)	1670.9	786.5	717.9
crystal size [mm]	0.15 × 0.30 × 0.30	0.30 × 0.40 × 0.40	0.40 × 0.30 × 0.25
crystal system	triclinic	triclinic	monoclinic
Z	2	4	4
space group (no.)	P $\bar{1}$ (2)	P $\bar{1}$ (2)	P2 ₁ /n (14)
a [Å]	15.614(4)	13.083(3)	13.197(5)
b [Å]	16.764(3)	16.824(4)	22.797(6)
c [Å]	19.596(4)	21.600(4)	13.835(5)
α [°]	108.81(1)	101.54(2)	90.00(0)
β [°]	97.78(2)	93.95(1)	97.92(3)
γ [°]	105.45(2)	92.63(1)	90.00(0)
V [Å ³]	4540(2)	4639(2)	4123(2)
ρ (calcd.) [g cm ⁻³]	1.339	1.251	1.290
T [K]	200	200	200
2θ range [°]	4.0–48.0	3.9–48.0	4.4–51.0
scan speed [° min ⁻¹]	ω = 12.0	ω = 10.0	ω = 10.0
no. rflns. measured	14472	14813	8015
no. unique rflns.	13886	14096	7668
no. reflns. obs.	7143	6693	5073
obs. criterion	I > 2σ(I)	I > 2σ(I)	I > 2σ(I)
no. of parameters	823	994	465
R _i (%)	8.9	8.1	5.5
R _w (%)	23.5	20.5	13.2
(refinement on F ²)			

and stirred under air for 5 h. The colour gradually changed to light-blue. The reaction was quenched by pouring the solution into 10 ml of an aqueous solution of NaCN (0.6 M). The organic solvent was evaporated and the aqueous phase was extracted with Et₂O (2 × 10 ml). The ethereal phase was dried with MgSO₄, filtered, and the solvent was evaporated to yield a white powder, which was analyzed by ³¹P-NMR spectroscopy.

1,1-Bis(diphenylphosphanomethyl)-1-(diphenylphosphorylmethyl)ethane [TriphosO, CH₃C(CH₂PPh₂)₂(CH₂P(O)Ph₂)]: The monoxide was either prepared by the method of Collman¹⁸ by oxidation of triphos in acetone with dilute H₂O₂ (30% yield), or isolated by chromatography of the triphosO/triphosO₂ mixture obtained from the General Procedure on silica gel (10 cm, Ø 2 cm) with ethyl acetate/benzene (1:1) as eluent; R_f(triphosO) = 0.75. – Yield: 190–290 mg (30–45%). – M.p. 126 °C (ref.¹⁸ 127–128 °C). – MS (EI); *m/z* (%): 640 (12) [M⁺], 563 (100) [M⁺ – Ph], 486 (6) [M⁺ – 2 Ph], 455 (6) [M⁺ – PPh₂], 439 (5) [M⁺ – OPPh₂], 425 (3) [M⁺ – CH₂OPPh₂]. – C₄₁H₃₉P₃O (640.7): calcd. C 76.86, H 6.14, P 14.50; found C 76.63, H 6.51, P 14.01.

1-(Diphenylphosphanomethyl)-1,1-bis(diphenylphosphorylmethyl)ethane [TriphosO₂, CH₃C(CH₂PPh₂)₂(CH₂P(O)Ph₂)₂]: The bisoxide was prepared according to the General Procedure, using 100 ml of THF instead of 40 ml. When the white powder was found to be contaminated with some triphosO (according to TLC or ³¹P NMR), this could be removed by chromatography on silica gel (10 cm, Ø 2 cm) with ethyl acetate/benzene (1:1) as eluent; R_f(triphosO₂) = 0.29. – Yield: 525–620 mg (80–95%). – M.p. 132 °C. – MS (EI); *m/z* (%): 656 (14) [M⁺], 578 (30) [M⁺ – Ph], 471 (15) [M⁺ – PPh₂], 455 (35) [M⁺ – OPPh₂], 441 (30) [M⁺ – CH₂OPPh₂]. – C₄₁H₃₉P₃O₂ (656.7): calcd. C 74.99, H 5.99, P 14.15; found C 74.87, H 6.20, P 14.05.

1,1,1-Tris(diphenylphosphorylmethyl)ethane [TriphosO₃, CH₃C(CH₂P(O)Ph₂)₃]: To a solution of triphos (1 mmol, 624 mg) in ace-

tone (30 ml) was added 2 ml of H₂O₂ (10%). The mixture was stirred for 6 h at room temperature and then the solvent was removed in vacuo. The white solid thus obtained was washed with H₂O and Et₂O/PE (2:1) and dried in vacuo. TLC (ethyl acetate/benzene, 1:1) showed only the presence of triphosO₃; R_f(triphosO₃) = 0.03. – Yield: 540 mg (80%). – M.p. 200 °C (ref.¹⁴ 198–200 °C). – MS (EI); *m/z* (%): 672 (5) [M⁺], 595 (12) [M⁺ – Ph], 519 (2) [M⁺ – 2 Ph], 471 (20) [M⁺ – OPPh₂], 457 (100) [M⁺ – CH₂OPPh₂]. – C₄₁H₃₉P₃O₃ (672.7): calcd. C 73.21, H 5.84, P 13.81; found C 73.11, H 6.16, P 13.13.

1,1,1-Tris(diphenylthiophosphorylmethyl)ethane [TriphosS₃, CH₃C(CH₂P(S)Ph₂)₃]. – *Method A*: To a solution of triphos (1 mmol, 624 mg) and CoCl₂ (0.1 mmol, 13 mg) in THF (40 ml) was added 150 mg of freshly sublimed *cyclo*-octasulfur (0.59 mmol). The suspension was sonicated until the sulfur dissolved. The resulting green solution was poured into 10 ml of an aqueous solution of NaCN (0.6 M). The organic solvent was evaporated and the aqueous phase was extracted with Et₂O (2 × 10 ml). The ethereal phase was dried with MgSO₄, filtered, and the solvent was evaporated to yield a yellow powder, which was recrystallized from CH₂Cl₂/EtOH to give white crystals of triphosS₃. Yield: 290 mg (40%).

Method B: To a solution of triphos (1 mmol, 624 mg) in THF (40 ml) was added 150 mg of freshly sublimed *cyclo*-octasulfur (0.59 mmol). The suspension was sonicated until the sulfur dissolved. The organic solvent was evaporated and the yellow powder was recrystallized from CH₂Cl₂/EtOH to give white crystals of triphosS₃. Yield: 400 mg (55%).

Elemental analysis indicated the presence of excess sulfur in the sample, which is not uncommon for reactions using *cyclo*-octasulfur¹⁷. No attempts were made to optimize the reactions to give purer samples of triphosS₃ as clean procedures for preparing this

ligand already exist.^[4] – M.p. 219 °C (ref.^[4] 211 °C). – MS (EI); *m/z* (%): 720 (23) [M⁺], 688 (35) [M⁺ – S], 656 (11) [M⁺ – 2 S], 624 (4) [M⁺ – 3 S], 611 (15) [M⁺ – S, – Ph], 578 (88) [M⁺ – 2 S, – Ph], 548 (38) [M⁺ – 3 S, – Ph]. – C₄₁H₃₉P₃S₃ (720.9): calcd. for C₄₁H₃₉P₃S₃·6: C 66.54, H 5.31, P 12.56, S 15.59; found C 66.22, H 5.40, P 12.55, S 15.29.

[η²-(*P,P*)-triphosO]CoCl₂ (4): To 1 mmol of CoCl₂ (130 mg) in THF (40 ml) was added 1 mmol of triphosO (640 mg), resulting in a dark-blue solution. The solution was slowly concentrated to ca. 8 ml yielding a blue precipitate, which was filtered off, washed with THF (3 × 8 ml) and Et₂O (4 × 10 ml) and dried in vacuo. Yield: 655 mg (85%). Crystals of (4)₂·CoCl₂ suitable for X-ray structural analysis were obtained after 3 weeks by vapor diffusion of Et₂O into a dilute solution of 4 in THF. – M.p. 156 °C. – C₄₁H₃₉Cl₂CoOP₃ (770.5): calcd. C 63.91, H 5.10, Cl 9.20, P 12.06; found C 63.61, H 5.48, Cl 8.82, P 11.65.

rac-[η²-(*P,O*)-triphosO₂]CoCl₂ (5). – *Method A*: To 1 mmol of CoCl₂ (130 mg) in THF (60 ml) was added 1 mmol of triphos (624 mg), resulting in a dark-blue solution. This was stirred under air for 6 h. The light-blue solution thus obtained was slowly concentrated to ca. 8 ml yielding a light-blue precipitate, which was filtered off, washed with THF (3 × 8 ml) and Et₂O (4 × 10 ml), and recrystallized from acetone/Et₂O. Yield: 470 mg (60%).

Method B: To 1 mmol of CoCl₂ (130 mg) in THF (60 ml) was added 1 mmol of triphosO₂ (657 mg), resulting in a light-blue solution. The solution was slowly concentrated to ca. 8 ml yielding a light-blue precipitate, which was filtered off, washed with THF (3 × 8 ml) and Et₂O (4 × 10 ml) and recrystallized from acetone/Et₂O. Yield: 630 mg (80%). Crystals of 5 suitable for X-ray structural analysis were obtained after 4 d by vapor diffusion of Et₂O into a dilute solution of the complex in acetone. – M.p. 226 °C (dec.). – C₄₁H₃₉Cl₂CoO₂P₃ (786.5): calcd. for 5·2 acetone: C 62.54, H 5.69; found C 61.18, H 5.63.

[(*P*(CH₃)₃)₄CoCl][BPh₄][7·(BPh₄)]. – *Method A*: To 0.5 mmol of 4 (385 mg) or 5 (393 mg) in 40 ml of THF was added solid NaBPh₄ (0.5 mmol, 171 mg). No colour change was observed. A solution of trimethylphosphane (0.5 ml, 1 M in THF) was then added, resulting in a colour change to bright-green. The organic solvent was evaporated. The solid residue was dissolved in 15 ml CH₂Cl₂ and filtered through 6 cm Kieselguhr to remove the NaCl. Recrystallization from CH₂Cl₂/Et₂O yielded a green powder. Yield: 55 mg (15%, based on Co). Dark-green crystals of 7·(BPh₄) suitable for X-ray structural analysis were obtained after 3 d by vapor diffusion of Et₂O into a solution of 7·(BPh₄) in CH₂Cl₂.

Method B: To 130 mg of CoCl₂ (1 mmol), dissolved in THF (40 ml), was added a solution of trimethylphosphane (4.5 ml, 1 M in THF) and solid NaBPh₄ (342 mg, 1 mmol), resulting in a colour change to bright-green. Recrystallization from THF/Et₂O yielded a green powder. Yield: 645 mg (90%). – M.p. 165 °C. – ESR (CH₂Cl₂, 295 K): *g*_{iso} = 2.14. – ESR (THF, 100 K): *g*_{av} = 2.11. – CV: *E*_p = –280 mV (irr.); *E*_p (reverse scan) = +210 mV; *E*_p = +990 mV (irr.). – C₃₆H₅₆BClCoP₄ (717.9): calcd. for 7·(BPh₄)·1 THF: C 60.81, H 8.17, Cl 4.49, P 15.68; found C 60.48, H 7.94, Cl 4.75, P 15.64.

* Dedicated to Professor H. Bärnighausen on the occasion of his 65th birthday.

[1] [1a] L. Horner, W. Jurgeleit, *Liebigs Ann. Chem.* **1955**, 591, 138–152. – [1b] K. Sasse (Ed.: E. Müller), *Methoden Org. Chem.* (Houben Weyl) **1963**, vol. XII/1, p. 140–145. – [1c] M.

Regitz (Eds.: H. Heydt, M. Regitz), *Methoden Org. Chem.* (Houben Weyl) **1982**, vol. E2, p. 41–43.

[2] [2a] K. Issleib, A. Brack, *Z. Anorg. Chem.* **1954**, 277, 254–270. – [2b] H. Gilman, G. E. Brown, *J. Am. Chem. Soc.* **1945**, 67, 824–826.

[3] [3a] R. K. Robins, B. E. Christensen, *J. Org. Chem.* **1951**, 16, 324–327. – [3b] C. Stuebe, W. M. LeSuer, G. R. Norman, *J. Am. Chem. Soc.* **1955**, 77, 3526–3529.

[4] E. Lindner, H. Beer, *Chem. Ber.* **1972**, 105, 3261–3270.

[5] [5a] S. A. Buckler, *J. Am. Chem. Soc.* **1962**, 84, 3093–3097. – [5b] M. B. Floyd, C. E. Boozer, *J. Am. Chem. Soc.* **1963**, 85, 984–986. – [5c] Y. Ogata, M. Yamashita, *J. Chem. Soc., Perkin Trans. 2* **1972**, 730–733. – [5d] H. W. Thompson, N. S. Kelland, *J. Chem. Soc.* **1933**, 1231–1236.

[6] [6a] D.-H. Chin, G. N. La Mar, A. L. Balch, *J. Am. Chem. Soc.* **1980**, 102, 5945–5947. – [6b] K. R. Dunbar, A. Quillevère, *Polyhedron* **1993**, 12, 807–819. – [6c] J. P. Birk, J. Halpern, A. L. Pickard, *J. Am. Chem. Soc.* **1968**, 90, 4491–4492. – [6d] G. Wilke, H. Schott, P. Heimbach, *Angew. Chem.* **1967**, 79, 62; *Angew. Chem. Int. Ed. Engl.* **1967**, 6, 92. – [6e] K. Takao, Y. Fujiwara, T. Imanaka, S. Teranishi, *Bull. Chem. Soc. Jpn.* **1970**, 43, 1153–1157. – [6f] A. Sen, J. Halpern, *J. Am. Chem. Soc.* **1977**, 99, 8337–8339.

[7] J. Ellermann, D. Schirmacher, *Chem. Ber.* **1967**, 100, 2220–2227.

[8] W. O. Siegl, S. J. Lapporte, J. P. Collman, *Inorg. Chem.* **1971**, 10, 2158–2163.

[9] K. Heinze, G. Huttner, L. Zsolnai, P. Schober, *Inorg. Chem.* **1997**, submitted.

[10] C. Mealli, S. Midollini, L. Sacconi, *Inorg. Chem.* **1975**, 14, 2513–2521.

[11] J. E. Huheey, *Anorganische Chemie*, de Gruyter, Berlin, New York, **1988**, p. 1072.

[12] F. Mani, M. Bacci, *Inorg. Chim. Acta* **1972**, 6, 487–490.

[13] [13a] F. A. Cotton, M. Goodgame, *J. Am. Chem. Soc.* **1961**, 83, 1777–1780. – [13b] F. A. Cotton, D. M. L. Goodgame, M. Goodgame, A. Sacco, *J. Am. Chem. Soc.* **1961**, 83, 4157–4161. – [13c] F. A. Cotton, O. D. Faut, D. M. L. Goodgame, R. H. Holm, *J. Am. Chem. Soc.* **1961**, 83, 1780–1785. – [13d] F. A. Cotton, D. M. L. Goodgame, M. Goodgame, *J. Am. Chem. Soc.* **1961**, 83, 4690–4699. – [13e] R. H. Holm, F. A. Cotton, *J. Chem. Phys.* **1959**, 31, 788–792.

[14] Co1: φ₁ (Co1–P11–C1–C4) –58.5; φ₂ (P11–C1–C4–C2) 64.3; φ₃ (C1–C4–C2–P12) –62.0; φ₄ (C4–C2–P12–Co1) 55.7; φ₅ (C2–P12–Co1–P11) –41.6; φ₆ (P12–Co1–P11–C1) 41.5; Co2: φ₁ –61.8; φ₂ 67.3; φ₃ –64.3; φ₄ 58.4; φ₅ –45.6; φ₆ 45.8; M. F. DaCruz, M. Zimmer, *Inorg. Chem.* **1996**, 35, 2872–2877.

[15]

$$\text{RMS} = \sqrt{\frac{1}{n} \sum_{i=1}^n [\alpha_i - 109^\circ]^2}; \alpha_i = \text{all X-Co-Y angles}; n = 6.$$

[16] K. Brandt, W. S. Sheldrick, *Chem. Ber.* **1996**, 129, 1199–1206.

[17] [17a] C. Bianchini, C. A. Ghilardi, A. Meli, A. Orlandini, *J. Organomet. Chem.* **1985**, 286, 259–270. – [17b] C. Bianchini, C. Mealli, A. Meli, M. Sabat, *Inorg. Chem.* **1984**, 23, 2731–2732.

[18] L.-K. Liu, *Acta Crystallogr.* **1988**, C4, 1402–1405.

[19] [19a] O. Alnagi, M. Zinoun, A. Glcizes, M. Dartiguenave, Y. Dartiguenave, *New J. Chem.* **1980**, 4, 707–709. – [19b] J. Ellermann, W. H. Gruber, *Z. Anorg. Allg. Chem.* **1970**, 364, 55–68.

[20] The equilibrium constants were determined in THF solutions by ³¹P-NMR spectroscopy.

[21] Higher concentrations of triphos could not be achieved as the solubility limit of the ligand in THF is reached at approximately 10^{–1} mol l^{–1}.

[22] D. D. Schmidt, J. T. Yoke, *J. Am. Chem. Soc.* **1971**, 93, 637–640.

[23] [23a] R. S. Drago, J. R. Stahlbush, D. J. Kitko, J. Brese, *J. Am. Chem. Soc.* **1980**, 102, 1884–1889. – [23b] N. W. Terry, E. L. Amma, L. Vaska, *J. Am. Chem. Soc.* **1972**, 94, 653–655. – [23c] J. Halpern, B. L. Goodall, G. P. Khare, H. S. Lim, J. J. Pluth, *J. Am. Chem. Soc.* **1975**, 97, 2301–2303. – [23d] O. M. Renaud, K. H. Theopold, *J. Am. Chem. Soc.* **1994**, 116, 6979–6980. – [23e] O. M. Renaud, G. P. A. Yap, A. L. Rheingold, K. H. Theopold, *Angew. Chem.* **1995**, 107, 2171–2173; *Angew. Chem. Int. Ed. Engl.* **1995**, 34, 2051–2052. – [23f] A. B. P. Lever, H. B.

- Gray, *Acc. Chem. Res.* **1978**, *11*, 348–355. — ^[23g] R. S. Drago, B. B. Corden, *Acc. Chem. Res.* **1980**, *13*, 353–360. — ^[23h] R. D. Jones, D. A. Summerville, F. Basolo, *Chem. Rev.* **1979**, *79*, 139–179. — ^[23i] L. Vaska, *Acc. Chem. Res.* **1976**, *9*, 175–183. — ^[23j] J. S. Valentine, *Chem. Rev.* **1973**, *73*, 235–245. — ^[23k] E. C. Niederhoffer, J. H. Timmons, A. E. Martell, *Chem. Rev.* **1984**, *84*, 137–203.
- ^[24] ^[24a] D. F. Evans, *J. Chem. Soc.* **1959**, 2003–2005. — ^[24b] T. H. Crawford, J. Swanson, *J. Chem. Educ.* **1971**, *48*, 382–386.
- ^[25] A. Muth, Diplomarbeit, University of Heidelberg, **1989**.
- ^[26] B. Heyn, B. Hipler, G. Kreisel, H. Schreer, D. Walther, *Anorganische Synthesechemie*, Springer Verlag, Berlin, Heidelberg, New York, London, Paris, Tokyo, **1986**.
- ^[27] ^[27a] G. M. Sheldrick, *SHELXS-86, Program for Crystal Structure Solution*, University of Göttingen, **1986**. — ^[27b] G. M. Sheldrick, *SHELXL-93, Program for Crystal Structure Refinement*, University of Göttingen, **1993**.
- ^[28] L. Zsolnai, G. Huttner, *XPMA, ZORTEP*, University of Heidelberg, **1997**.

[97139]